



Design and Optimization of Manufacturing Process of Polymer Composites Through Multiscale Cure Analysis and NSGA-II

Yagnik Kalariya¹ · Soban Babu Beemaraj¹ · Amit Salvi¹

Received: 6 August 2023 / Accepted: 26 September 2023 / Published online: 3 November 2023
© The Minerals, Metals & Materials Society 2023

Abstract

Thermoset polymer composite structures are heavily used in the aerospace, defense, transport, and energy sectors due to their lightweight and high-performance behavior. Thermoset polymer resins require external heat for manufacturing/curing. The behavior of these polymer composite materials is highly dependent on curing process as it affects evolution of material properties as well as residual stresses and deformation. Various cure process parameters, mainly related to cure thermal cycle, need to be optimized to get the desired properties of these structures. In this paper, the polymer cure process is explicitly modeled through finite element method. Its effects at the structural level are captured by modeling thermo-chemical-mechanical analysis through multiple length scales. The multi-scale analysis is carried out by surrogate models to reduce run time. In this study, non-dominated sorting genetic algorithm II is used for multi-objective cure process optimization. The objectives are to minimize the spring-in angle and minimize the process time with achieving degree of cure above given requirement. Insights from such optimization can be utilized by product designers as well as manufacturers to take timely decisions to improve the performance of these composite structures.

Keywords Thermoset polymer composites · Cure kinetics · Multi-scale method · Finite element analysis · Genetic algorithm · NSGA-II

Introduction

Fiber-reinforced thermoset polymer composites find extensive applications in the aerospace, defense, transport, and energy industries due to their lightweight and high-performance characteristics [1–4]. Characteristics of these composite materials are governed by their constituent materials, lay-up orientation, manufacturing process, etc. The manufacturing (curing) process of thermosetting polymer requires

heating a mixture of resin and hardener at elevated temperature to form the cross linking [5–7]. This curing process results from a combination of externally applied heat and local heat generation due to exothermic reactions [8]. During curing, phase transformation occurs, transforming the resin from a liquid to a solid state and achieving the final mechanical properties. However, the curing process also induces cure shrinkage and thermal strains due to the applied temperature cycle, leading to residual stresses and deformations. Often, the effects of the manufacturing process are overlooked in the design of composite structures, significantly impacting their structural performance. Moreover, inadequate temperature control during curing can result in cure gradients in the resin, making the characteristics of the final cured part highly dependent on the curing process and applied temperature cycle [9–11]. The cure temperature cycle of the resin is usually provided by the resin manufacturer as the Manufacturer Recommended Cure Cycle (MRCC), which is typically based on experiments conducted for virgin resin. However, the cure process parameters need to be adjusted for specific composite parts with varying fiber architectures. Applying

Soban Babu Beemaraj and Amit Salvi have contributed equally to this work.

✉ Soban Babu Beemaraj
soban.bb@tcs.com

Yagnik Kalariya
yp.kalariya@tcs.com

Amit Salvi
salvi.amit@tcs.com

¹ TCS Research, Tata Consultancy Services Limited, Pune, Maharashtra 411013, India

the MRCC to parts with complex geometries and fiber architectures induces process-induced stresses at different length scales [12, 13], leading to part-level deformations [14–17].

This paper presents the development of an Integrated Computational Materials Engineering (ICME)-based multi-scale approach for simulating the composite curing process. It can be used to analyze the behavior of composite structure during and post manufacturing, encompassing calculations of deformation, spring-in angle, residual stress, temperature gradient, and Degree of Cure (DoC). The proposed approach is coupled with mathematical optimization, utilizing the Non-dominated Sorting Genetic Algorithm II (NSGA-II), to achieve simultaneous minimization of the spring-in angle and process time for L-channel. Additionally, the optimization process ensures that the minimum DoC requirement is satisfied during the curing process.

Composite structures exhibit a multi-scale nature, where the scales of their constituents (fibers and resin) are considerably smaller than the resulting structure. The prediction of responses for such structures presents substantial complexity due to the intricate architecture and orientations of fibers at multiple length scales. Analyzing these structures necessitates coupling the microscopic model with the macroscopic model. Multi-scale methods facilitate the calculation of effective composite properties based on the constituent properties and micro-structure; a process known as homogenization. Moreover, these methods enable the analysis of responses at lower length scales for critical locations in the part level, termed localization. Various authors developed multi-scale methods for composite materials to model thermal and mechanical responses at material and part level [18]. There are analytical and semi-analytical multiscale approaches which are simpler to implement and computationally efficient. However, it lacks generality and limits to specific use cases. Özdemir et al. [19] used FE² computational homogenization approach for thermo-mechanical analysis of heterogeneous solids. It is an integrated or explicit multiscale approach involving Finite Element Analysis (FEA) at two length scales. The actual response at each material point in the given part is calculated on-demand running lower length scale analysis. The multiscale approach has also been extended to calculate process induced stresses and deformation due to curing. Mahnken et al. [20] employed three scale sequential FEA framework to calculate the homogenized properties from micro-scale to macro-scale and utilized it at part level. In addition, Chen et al. [21] extended the multi-scale model to study the stress and deformation at the part level. Recently, Zhi et al. [22] also used explicit multiscale approach to analyze the cure induced deformation. While explicit methods can produce the results accurately, they are expensive in terms of computational cost and time. It is required to run multiple

simultaneous microscale analysis, each one for a material point at part level. In the case of cure process simulation being a transient analysis, it is even more expensive. Therefore, these explicit methods might not be effective in early-stage optimization studies because typical optimization methods require a large number of functional evaluations. In these circumstances, need an effective method that reduces the computational burden without sacrificing the accuracy. One such alternative is to use low-cost surrogate models in lower length scales. For example, Wang et al. [23] have used exponential function as surrogate model to fit the evolution of properties and cure shrinkage at meso-scale and used at part level. There remains the scope of improvement and exploration in surrogate assisted multi-scale cure process analysis.

Several researchers combined the FEA with multiple optimization algorithms, such as iterative numerical method [24], simulated annealing and Nelder-Mead algorithm [25], Genetic Algorithm (GA) [26], to minimize process time. A significant amount of reduction in process time is reported for thick and ultra-thick composite parts compared to MRCC. The single objective optimization is relatively easy to perform, but real-world problems require handling multiple conflicting objectives. Approaches like NSGA-II [27] can be employed to optimize the multi-objective cure problem. Struzziero and Skordos [28] optimized the temperature overshoot and total cycle time using the Multi-Objective Genetic Algorithm (MOGA) and FEA. Dolkun et al. [29] used MOGA-2 with FEA to optimize the maximum temperature difference, maximum degree of cure difference, and total cure time. Zhang et al. [30] and Hui et al. [31] used NSGA-II with FEA in multi-objective optimization. The former one minimizes the maximum temperature difference and total cure time, and the latter one minimizes the maximum temperature gradient, maximum residual stress, and process time.

From extensive literature survey, it can be concluded that authors developed explicit multi-scale methods and optimization methods independently. These methods are not used to guide the manufacturers to select the cure cycle for the given composite part. This paper proposes a solution approach that utilizes the in-house developed ICME framework combined with surrogate assisted multiscale finite element analysis and NSGA-II to design the manufacturing process for thermoset polymer composites. The novelty of the proposed approach is using surrogate assisted multiscale finite element analysis within NSGA-II to concurrently optimize conflicting objectives while considering different design requirements. The developed surrogate assisted multi-scale finite element analysis is computationally efficient compared to the explicit finite element analysis. In addition, this approach reduces the computational time enormously while designing the manufacturing process. The

proposed approach applied to L-channel composite structure to minimize the process time and spring-in angle while considering DoC above the required limit.

The paper is organized as follows. Section “**Solution Approach for Process Optimization**” explains the developed multi-scale approach and optimization strategy for process optimization of composite structures. Use case problem and associated results are discussed in Sect. “**Problem Definition**” and Sect. “**Results and Discussions**”, respectively. Finally, conclusions are provided in Sect. “**Conclusions**”.

Solution Approach for Process Optimization

Cure kinetics is modeled through finite element method to analyze the cure effects of resin on composite material. It essentially includes development of cure model, modeling the evolution of properties during cure, and cure shrinkage and corresponding stress development. It is achieved through including lower length scale models to calculate the homogenized properties from its constituents’ properties. Finally, a cure process simulation model at part level is developed to analyze the process and subsequently optimized through genetic algorithm.

Cure Kinetics

Analyzing the cure process, i.e., a crosslinking reaction, requires coupled modeling of thermo-chemical-mechanical analysis where the material properties evolve as cure process progresses. The progress of cure process is often measured as DoC, and it varies from 0 to 1. The degree of cure increases monotonically as per given time and temperature, and it reaches 1 once it gets fully cured. Degree of cure is defined as (refer Eq. (1)),

$$\phi = \frac{1}{H_r} \int_0^t \frac{dq}{dt} dt \quad (1)$$

where $\frac{dq}{dt}$ and H_r are rate of heat generation and total heat released during the cure process, respectively. H_r is also called heat of reaction. DoC is defined as the ratio of the total heat released till time t to the heat of reaction. The rate of heat generation can be determined using Eq. (2).

$$\frac{dq}{dt} = \frac{d\phi}{dt} (1 - V_f) \rho_r H_r \quad (2)$$

where $\frac{d\phi}{dt}$, V_f , and ρ_r are rate of degree of cure, volume fraction of fiber, and density of resin, respectively. The cure kinetics is often modeled like phenomenological models

proposed by Kamal [32]. Here, the rate of degree of cure follows Arrhenius type equation, and it is given in Eq. (3).

$$\frac{d\phi}{dt} = \frac{K\phi^m(1-\phi)^n}{1 + e^{C(\phi - (\phi_{c0} + \phi_{CT}T))}} \quad (3)$$

where K , m , n , and T are Arrhenius constant, first and second exponent constants, and temperature, respectively. Whereas C , ϕ_{c0} , and ϕ_{CT} are constants accounting for correction due to diffusion and slowing down rate of DoC at given temperature [33]. The Arrhenius constant is defined as (refer Eq. (4)).

$$K = A \exp\left(\frac{-\Delta E}{RT}\right) \quad (4)$$

where A , ΔE , and R are frequency constant, activation energy, and universal gas constant, respectively.

As mentioned earlier, the curing process for epoxy resins needs external heating, and DoC is a function of temperature cycle. Figure 1 shows the evolution of degree of cure for isothermal cure process at various temperature of epoxy 8552. As the applied temperature increases, the cure process accelerates, leading to a higher degree of cure achieved. The thermal and mechanical properties also evolve as cure progresses. Figure 2 represents the evolution of viscosity and shear modulus. At the start of curing, resin will be in liquid phase. As the curing process progresses, the viscosity steadily increases, reaching a gel point where the material gradually transitions toward a solid phase. Simultaneously, the shear modulus evolves from nearly zero to its final value at the completion of the curing process. The evolution of the properties depends on the degree of cure and hence temperature. This evolution becomes complex to model for thermoset composites due to the presence of fiber and its architecture and its orientation at different length scales. Therefore, it is required to build lower length scale models for composites and extract or homogenize these properties to use it at part levels.

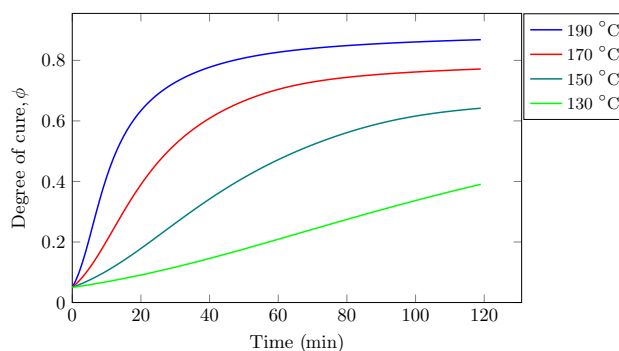


Fig. 1 Degree of cure evolution for isothermal cure processes of epoxy 8552

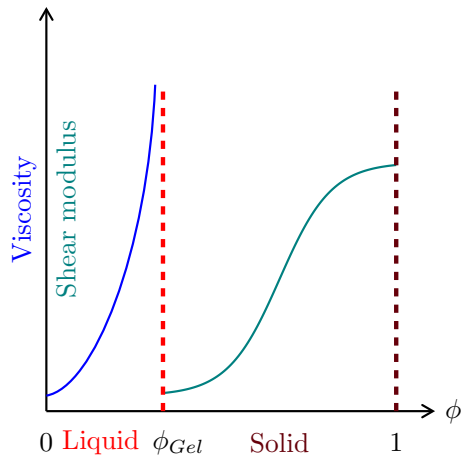


Fig. 2 Evolution of viscosity and shear modulus with degree of cure

Multiscale Method

Figure 3 depicts the workflow to extract the evolving properties from its constituents as homogenized during the cure. It starts with building a lower length scale model, micro-scale, as Representative Volume Element (RVE) for a given material system. It carries out virtual testing to characterize and subsequently homogenize the material properties. The lowest length scale involves the analysis of RVE of unidirectional lamina having fiber and resin as two separate constituents such a RVE is shown in Fig. 4. The volume fraction of fiber and fiber arrangement is critical at this length scale. Currently, the elastic properties and behavior and thermal conductivity are calculated through computational homogenization scheme using FEA. These homogenized properties are

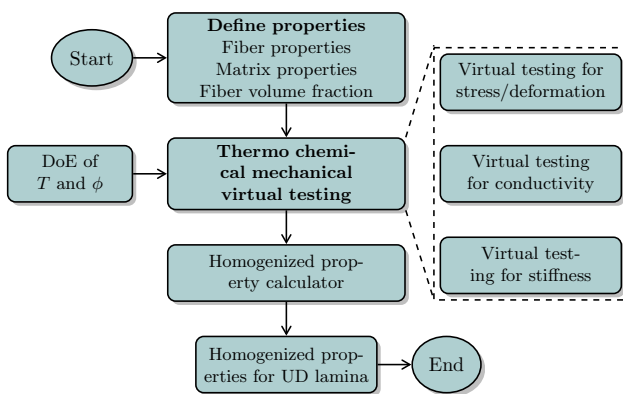


Fig. 3 Workflow to obtain the evolution of homogenized properties for composites due to curing

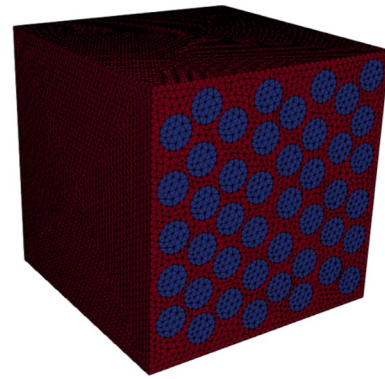


Fig. 4 RVE for uni-directional composite lamina

employed in later stages of analysis and optimization for the composite material system.

The Fourier’s law of heat conduction and heat transfer analysis is used to calculate the homogenized conductivity for composites. The constitutive relationship between heat flux \mathbf{q}'' , conductivity \mathbf{k} , and temperature gradient ∇T is given by,

$$\mathbf{q}'' = -\mathbf{k} \cdot \nabla T \tag{5}$$

The average heat flux $\langle \mathbf{q}'' \rangle$ for the RVE can be calculated as,

$$\langle \mathbf{q}'' \rangle = \frac{1}{V_R} \int_R \mathbf{q}'' dV \tag{6}$$

The homogenized thermal conductivity can be calculated from,

$$\langle \mathbf{q}'' \rangle = -\mathbf{k}_e \cdot \langle \nabla T \rangle \tag{7}$$

The homogenized conductivity for all three directions is calculated applying unit temperature gradient across the opposite faces of RVE in three separate virtual tests. Homogenized thermal conductivity is equal to the average heat flux for the direction in which temperature gradient is applied.

For extracting homogenized elastic properties, three virtual tests are required assuming the UD composite material as transverse isotropic material [34]. These are one in-plane shear and two normal strain tests with unit value. Generalized Hooke’s law is used to calculate the effective elastic tensor and given as,

$$\langle \sigma \rangle = \langle C \rangle \langle \epsilon \rangle \tag{8}$$

where $\langle C \rangle$ is the effective elastic stiffness tensor (fourth-order tensor) that describes the material’s elastic properties. $\langle \epsilon \rangle$ is the strain tensor due to externally applied loads. In this case, unit strain is applied to RVE through periodic boundary conditions. The resultant stresses are volume averaged

to get the effective elastic stiffness tensor for the total three strain tests as mentioned earlier.

With this setup of FEA, Design of Experiments (DoE) is carried out at different degrees of cure and temperature. The combined response later is used to get the surrogate models with respect to degree of cure and temperature. The other properties such as density and specific heat are homogenized through the rule of mixture.

Calculation of homogenized cure shrinkage and thermal strain is difficult for composites material. Due to fiber-matrix interactions, homogenized cure shrinkage not only depends on resin cure shrinkage but also on resin and fiber elastic constants [35]. Similarly, homogenized thermal strain additionally depends on resin and fiber elastic constants other than temperature and thermal co-efficient of expansion. Explicit multiscale approach can be helpful here to calculate complex response at local microstructure accurately without summarizing its constitutive behavior. However, it lacks computational efficiency. One way to address this bottleneck is to create surrogate models of target response. The generalized Hooke’s law with residual stresses is given in Eq. (9).

$$\sigma = C\varepsilon + \sigma^{\text{res}} \tag{9}$$

where σ^{res} is the cure process induced residual stress, it can be calculated using Eq. (10). This relation remains valid till part gets cured and demolded.

$$\sigma^{\text{res}} = C(T, \phi)(\varepsilon^{\text{th}}(T, \phi) + \varepsilon^{\text{cs}}(\phi)) \tag{10}$$

In this case, the cure shrinkage ε^{cs} and thermal strains ε^{th} induces stresses. Instead of creating separate surrogate models for cure shrinkage and thermal strain first and then calculate stresses from it with elastic constants, authors suggest creating surrogate model for these stresses directly if possible and utilize in user subroutine USERMAT. It can avoid possible error propagation from any errors in individual surrogate models of elastic constants, cure shrinkage, and thermal strain. These residual stresses are a function of temperature and degree of cure. The second order polynomial regression is carried out to create surrogate models of the stresses as a function of temperature and degree of cure as shown in Eq. (11).

$$\sigma^{\text{res}} = f(\mathbf{x}) \approx c_0 + \sum_{i=1}^2 c_i x_i + \sum_{i=1}^2 \sum_{j \geq i}^2 c_{ij} x_i x_j \tag{11}$$

where x_1 and x_2 are temperature, T , and DoC, ϕ , respectively. c_0 , $c_{i|i=1:2}$ and $c_{ij|i=1:2, j=i:2}$ are coefficients of polynomial that need to be found using the data from the micro-scale RVE simulation.

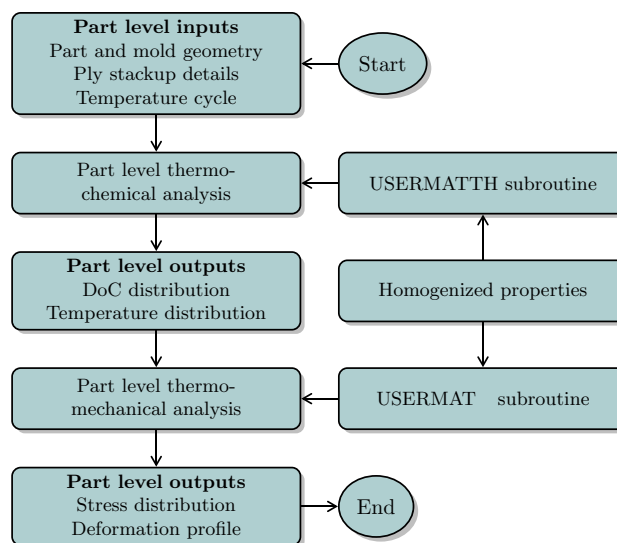


Fig. 5 Workflow of finite element model for cure process analysis of composite part

Simulation of Cure Process Analysis Through FEM

The process analysis is carried out in ANSYS Mechanical APDL through user subroutines. The workflow of this process simulation is shown in Fig. 5. The meshed part and mold geometry is provided as an input with ply stack-up and cure thermal cycle. All required homogenized properties for composites are defined in user subroutines. The whole analysis is divided into two sequentially coupled analysis: thermo-chemical and thermo-mechanical. In the former one, temperature is applied as per given thermal cycle with respect to time and calculates the evolution of temperature and degree of cure field for the whole model over time. The governing equation for heat transfer in thermal analysis, a transient Fourier anisotropic heat conduction equation with a heat generation from resin curing, is given as:

$$\rho c \frac{\partial T}{\partial t} = \frac{\partial}{\partial x_i} \left(k_{ij} \frac{\partial T}{\partial x_j} \right) + (1 - V_f) \rho_r H_r \frac{\partial \phi}{\partial t} \quad (i, j = 1, 2, 3) \tag{12}$$

where ρ , c and k_{ij} are homogenized density, specific heat, and thermal conductivity tensor for given composite, respectively. Density and specific heat for composites are calculated as per rule of mixture from its constituents whereas thermal conductivity in all three directions are extracted through computational homogenization which is explained in Section “Multiscale Method”. The homogenized thermal conductivity in three directions, specific heat, and cure model are defined in user subroutine USERMATTH.

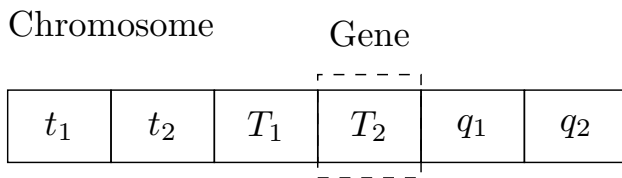


Fig. 6 Chromosome representation of design variables

The complete evolution of these temperature and degree of cure fields over time are forwarded to thermo-mechanical analysis as an input with required mechanical properties. The governing equation for the analysis is stress equilibrium and expressed as,

$$\frac{\partial \sigma_{ij}}{\partial x_i} + f_j = 0 \quad (j = 1, 2, 3) \quad (13)$$

where σ_{ij} is the total stress tensor, and f_j is the body force acting on the material.

Various constitutive models are available to represent the evolution of mechanical properties of composites during cure [36]. In the presented study, the mechanical properties are evolved as per Cure-Hardening Instantaneous Linear Elastic (CHILE) method. In this method, the material is considered to have elastic behavior and instantaneous elastic modulus at each time depending on temperature and degree of cure [37]. It changes over time as the cure progresses. The homogenized mechanical properties are defined in user subroutine USERMAT where one needs to define elastic stiffness tensor and update stresses based on the given temperature and degree of cure and previous state. The modeling of the interaction between mold and part is critical and significantly affects the final outputs of the analysis [38]. The sliding type of contact interaction between mold and part is created based on multi-point constraint algorithm for the current study. Separation between mold and part is not allowed during the curing process. After the cure process get completed, mold elements are killed in finite element analysis to replicate the demolding process. The analysis gives the accumulated residual stresses and deformation as an output before and after demolding.

This FEA model is required to work as a black box which can evaluate the objectives and constraints as per given input variables in optimization setup. It needs to be parameterized and automated for post-processing as per the optimization problem. The post-processing is carried out through pyANSYS [39] to simplify the extraction of required values.

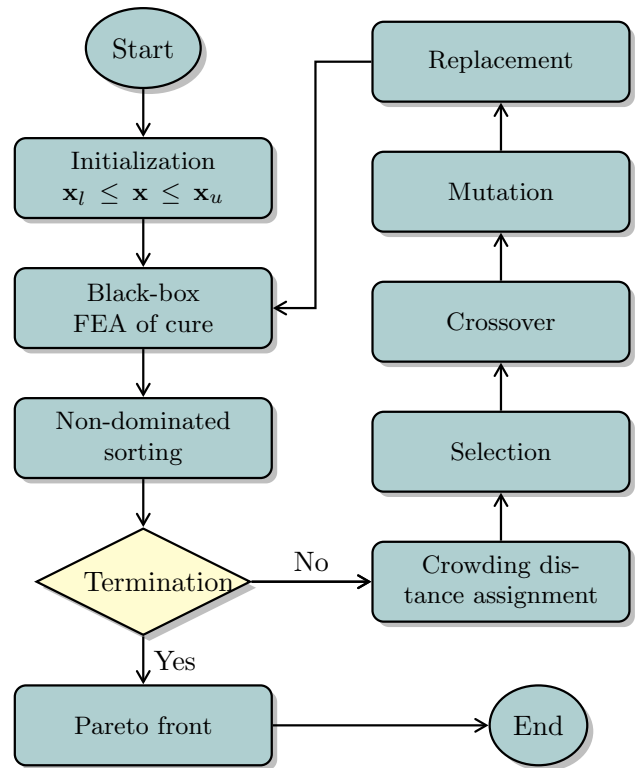


Fig. 7 NSGA-II workflow

Process Optimization Through NSGA-II

In this paper, NSGA-II is used to find the Pareto front. NSGA-II is a derivative free global optimization technique based on Charles Darwin's theory of natural evolution [40] with modified mating and survival selection. NSGA-II involves converting decision variables/input variables into chromosomes (refer Fig. 6). The optimizer starts with initial population (set of solutions), and successive solutions are created using genetic operations such as crossover and mutation until it reaches termination criterion. Figure 7 explains the work flow of NSGA-II optimization operation. It starts with an initial population such as random number generator or latin hypercube sampling. Current populations are evaluated against the objective functions using the block-box simulation. The current population is ranked based on the non-dominated sorting algorithm. The solution is said to dominate another if it is better in at least one objective and not worse in any other objective. If the number of block-box simulation exceeds the predefined limit, the algorithm stops otherwise crowding distance is assigned to each solution in the non-dominated fronts to maintain diversity. In the selection stage, non-dominance rank and crowding distance are used. Solutions with higher ranks and greater crowding

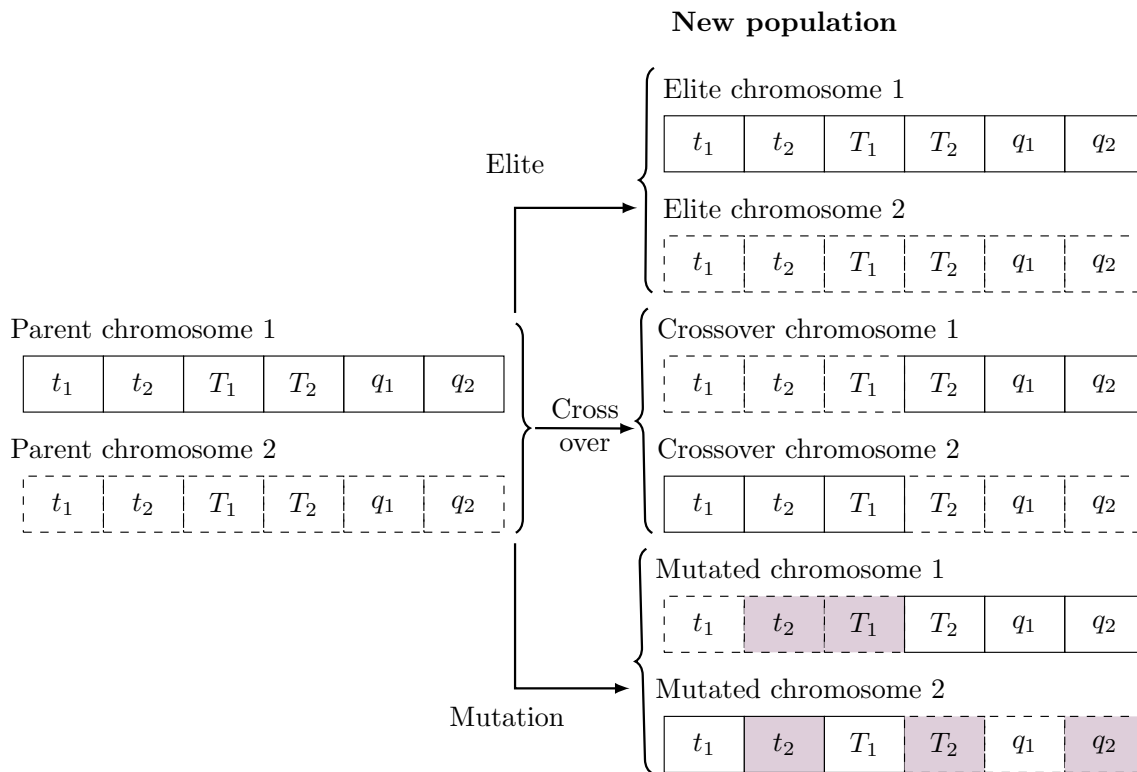


Fig. 8 Genetic operation on design variables

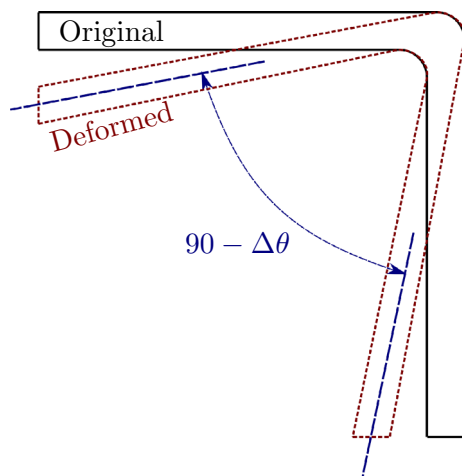


Fig. 9 Spring-in deformation in L-channel

distances are preferred to maintain diversity. The selected solutions are genetically modified using the crossover and mutation operation (see Fig. 8). Genetically modified solutions are known as offspring. During the replacement process, the generated offspring replaces the existing solutions.

Problem Definition

Angular channels or L-channels made of composites are often used as principal load bearing structural part. Spring-in angle, $\Delta\theta$, (refer Fig. 9) is often observed in these channels post manufacturing which becomes a concern during assembly [41]. It can affect structural performance during the service life if assembled forcefully. With focus on this problem, the objective is to design temperature cycle, often called cure thermal cycle, for curing process of thermoset polymer composite which minimizes process time and spring-in angle for L-channel. To maintain the desirable mechanical properties, it should also reach the DoC at least up to 0.8. The two objectives, process time and spring-in angle, are highly conflicting in nature. In these circumstances, there is no single optimal solution instead the goal is to find the set of Pareto optimal solutions such that any improvement in one objective means deteriorating another. For the concise understanding of problem, word formulation from McDowell et al. [42] is used, and it is shown as follows:

Multi-objective cure optimization problem

Given:

- Mold and part geometry
- Ply stacking sequence
- Ply thickness
- Ply material: fiber and matrix
- Fiber volume fraction
- Bounds for the heat cycle parameter

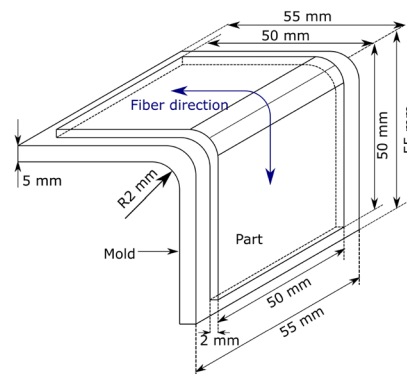
Find:

- Heat cycle parameters
 - Dwell times: t_1 and t_2
 - Dwell temperatures: T_1 and T_2
 - Heating rates: q_1 and q_2

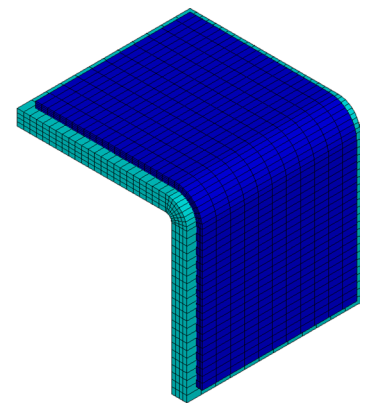
Satisfy:

- **System goals:**
 - Minimize the total process time, t_p (min)
 - Minimize the spring-in angle, $\Delta\theta$ ($^\circ$)
- **System constraints:**
 - The minimum DoC in the part should be at least above 0.8

Fig. 10 Mold and part geometry considered in this study



(a) Mold and part geometry dimension



(b) FE mesh of the mold and part

Table 1 Mesh detail for the FEA of mold and part

	Number of elements	Number of nodes	Thermal analysis	Mechanical analysis
Mold	2640	3640	SOLID278	SOLID185
Part	2464	3420	SOLID278	SOLID185

Table 2 Properties of Invar material used for mold

Property	Value
Density (kg m ⁻³)	8100
Specific heat capacity (J kg ⁻¹ K ⁻¹)	515
Thermal conductivity (W m ⁻¹ K ⁻¹)	11
Young’s modulus (GPa)	142
Poisson’s ratio	0.3
CTE (μm m ⁻¹ K ⁻¹)	1.3

Table 3 Properties of AS4 fiber

Property	Value
Density (kg m ⁻³)	1790
Specific heat capacity (J kg ⁻¹ K ⁻¹)	931 + 3.47T
Longitudinal thermal conductivity (W m ⁻¹ K ⁻¹)	2.4 + 5.07 × 10 ⁻³ T
Transverse thermal conductivity (W m ⁻¹ K ⁻¹)	7.69 + 1.56 × 10 ⁻² T
Longitudinal Young’s modulus (GPa)	221
Transverse Young’s modulus (GPa)	17.25
In-plane Poisson’s ratio	0.2
Transverse Poisson’s ratio	0.25
In-plane shear modulus (GPa)	27.6
Transverse shear modulus (GPa)	6.89
Longitudinal CTE (μm m ⁻¹ K ⁻¹)	-0.9
Transverse CTE (μm m ⁻¹ K ⁻¹)	7.2

Table 4 Cure kinetics parameters of epoxy 8552 [33]

Parameters	Value
A (s ⁻¹)	7.0 × 10 ⁴
m	0.5
n	1.5
C	30
φ _{c0}	-1.515
φ _{cT} (K ⁻¹)	5.171 × 10 ⁻³
ΔE (J mol ⁻¹)	6.5 × 10 ⁴
H _R (J kg ⁻¹)	5.74 × 10 ⁵
T _g (K)	268 + 220φ

The mold and part geometry is illustrated in Fig. 10a. Where mold’s two flanges are having length and breadth of 55 mm and fillet radius of 2 mm. Part’s two flanges are having length and breadth of 50 mm. The mold and part thickness is 5 mm and 2 mm, respectively. The mold is made up of Invar material. The entire part is made up of AS4/8552 unidirectional

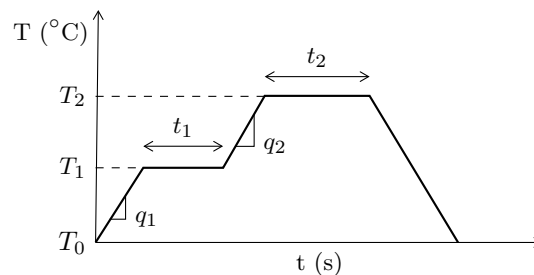


Fig. 11 Heat cycle definition

lamina. Here, fiber volume fraction is 0.573. The cure simulation model is constructed using Ansys Mechanical APDL tool. The meshed model is shown in Fig. 10b and associated FE mesh details are given in Table 1. The temperature as per cure thermal cycle is applied at the bottom surface of mold and it is constrained completely during the cure process. The properties of Invar are listed in Table 2. The properties of constituents for AS4/8552 composites are taken from earlier work of Johnston [43]. The properties of AS4 fiber are listed in Table 3. The values of cure kinetics parameters are listed in Table 4.

The evolution of epoxy 8552 resin modulus is given by Eq. (14). It is defined in the form of CHILE model as explained earlier in Section “Simulation of Cure Process Analysis Through FEM”.

$$E_r = \begin{cases} E_r^0 & T^* < T_{c1} \\ E_r^0 + \left(\frac{T^* - T_{c1}}{T_{c2} - T_{c1}} \right) (E_r^\infty - E_r^0) & T_{c1} < T^* < T_{c2} \\ E_r^\infty & T^* > T_{c2} \end{cases} \quad (14)$$

where T* is defined as

$$T^* = T_g - T \quad (15)$$

In Eq. (14) E_r⁰ and E_r[∞] are uncured and fully cured resin modulus having values 4.67 MPa and 4.67 GPa, respectively. T_{c1} and T_{c2} are critical temperatures at which resin modulus starts and stops evolving. Their values are -45.7 K and -12 K, respectively. T_g is glass transition temperature.

The volumetric cure shrinkage for the resin depends on DoC and calculated through Eq. (16) given as follows:

$$V_r^S = \begin{cases} 0 & \phi < \phi_{c1} \\ AC_s + (V_r^{S\infty} - A)C_s^2 & \phi_{c1} < \phi < \phi_{c2} \\ V_r^{S\infty} & \phi > \phi_{c2} \end{cases} \quad (16)$$

where C_s is defined as

$$C_s = \frac{\phi - \phi_{c1}}{\phi_{c2} - \phi_{c1}} \quad (17)$$

ϕ_{c1} and ϕ_{c2} in Eq. (16) are critical DoC values at which resin starts and stops shrinking. Their values are 0.055 and 0.651. The final volumetric cure shrinkage $V_r^{S\infty}$ is 0.099. The value of factor A to account nonlinearity of shrinkage with DoC is 0.173.

In this study, two step parameterized temperature cycle is used for process optimization as shown in Fig. 11. Where T_0 , T_1 , and T_2 are room temperature and first and second dwell temperature, respectively. q_1 and q_2 are two heating rates, and t_1 and t_2 are first and second dwell time, respectively. These six input variables are used for parameterization, and its bounds are given in Table 5. Since one of the objectives is to minimize the process time, higher bounds of dwell time and lower bounds of heating rates are kept same as those of MRCC. Keeping in mind the thickness of L-channel and possibility temperature gradient, the higher bound of heating rates are kept at $3\text{ }^\circ\text{C min}^{-1}$. The degree of cure achieved is highly dependent on second dwell temperature. Therefore, higher values from $160\text{ }^\circ\text{C}$ to $180\text{ }^\circ\text{C}$ is taken.

Table 5 Bounds of the 2-step heat cycle

Parameter	Minimum	Maximum
t_1 (min)	0	60
t_2 (min)	30	120
T_1 ($^\circ\text{C}$)	110	160
T_2 ($^\circ\text{C}$)	160	180
q_1 ($^\circ\text{Cmin}^{-1}$)	1	3
q_2 ($^\circ\text{Cmin}^{-1}$)	1	3

Results and Discussion

This study employs the surrogate-assisted multi-scale method to simulate the spring-in angle and process time for an L-channel composed of AS4/8552 composite uni-directional lamina. The validation of generated surrogate models for stress at micro-level is presented in this section, followed by the discussion of the optimization study, which combines the surrogate-assisted multi-scale method with NSGA-II.

The homogenized elastic constants are calculated through DoE as explained in Section “Multiscale Method” for the given composites through FEA in ANSYS APDL. The evolution of these elastic constants with DoC during curing is shown in Figs. 12 and 13 for epoxy 8552 and AS4/8552, respectively. For generating the surrogate models for residual stresses, the cure temperature cycle is parameterized using heating rates, dwell times, dwell temperatures. The Latin hypercube sampling is used to sample these parameters to define multiple temperature cycles with same bounds of input variables as given in Table 5. The output stress data are extracted from performing virtual tests on RVE with these generated cure temperature cycles. All sides of RVE are constrained completely and applied temperature as per cure cycle. The resultant stresses at specific intervals are extracted and volume averaged. This average stress along with temperature and degree of cure is used to construct the surrogate model as discussed in Section Multiscale Method. The input training data with constructed surrogate models are shown in Fig. 14 for stress along the fiber direction (refer Fig. 14a and b), σ_{11} , and stress transverse to the fiber direction (refer Fig. 14c and d), σ_{22} . Here, σ_{33} is not shown, and it is similar to σ_{22} because of equal thermal and cure shrinkage strains along with transversely isotropic

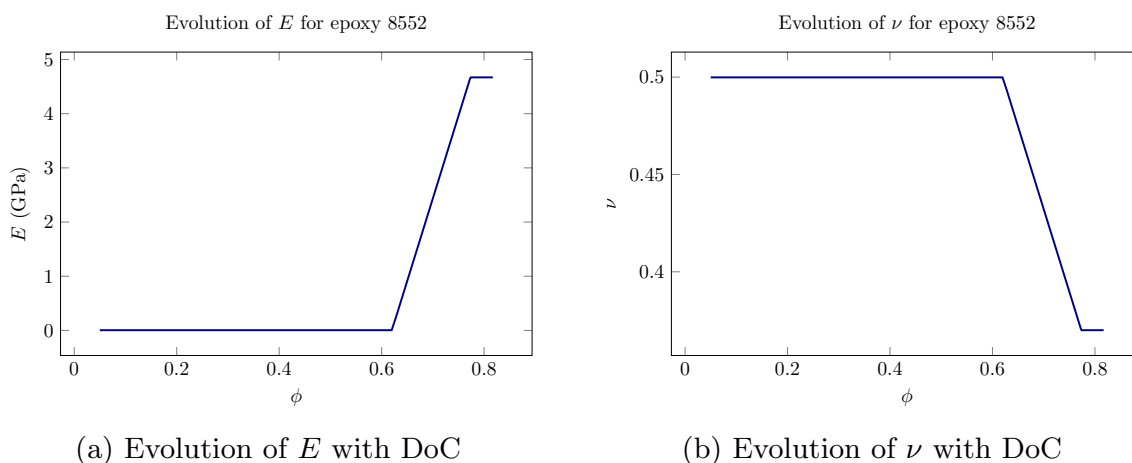


Fig. 12 Evolution of elastic constants with DoC for epoxy 8552

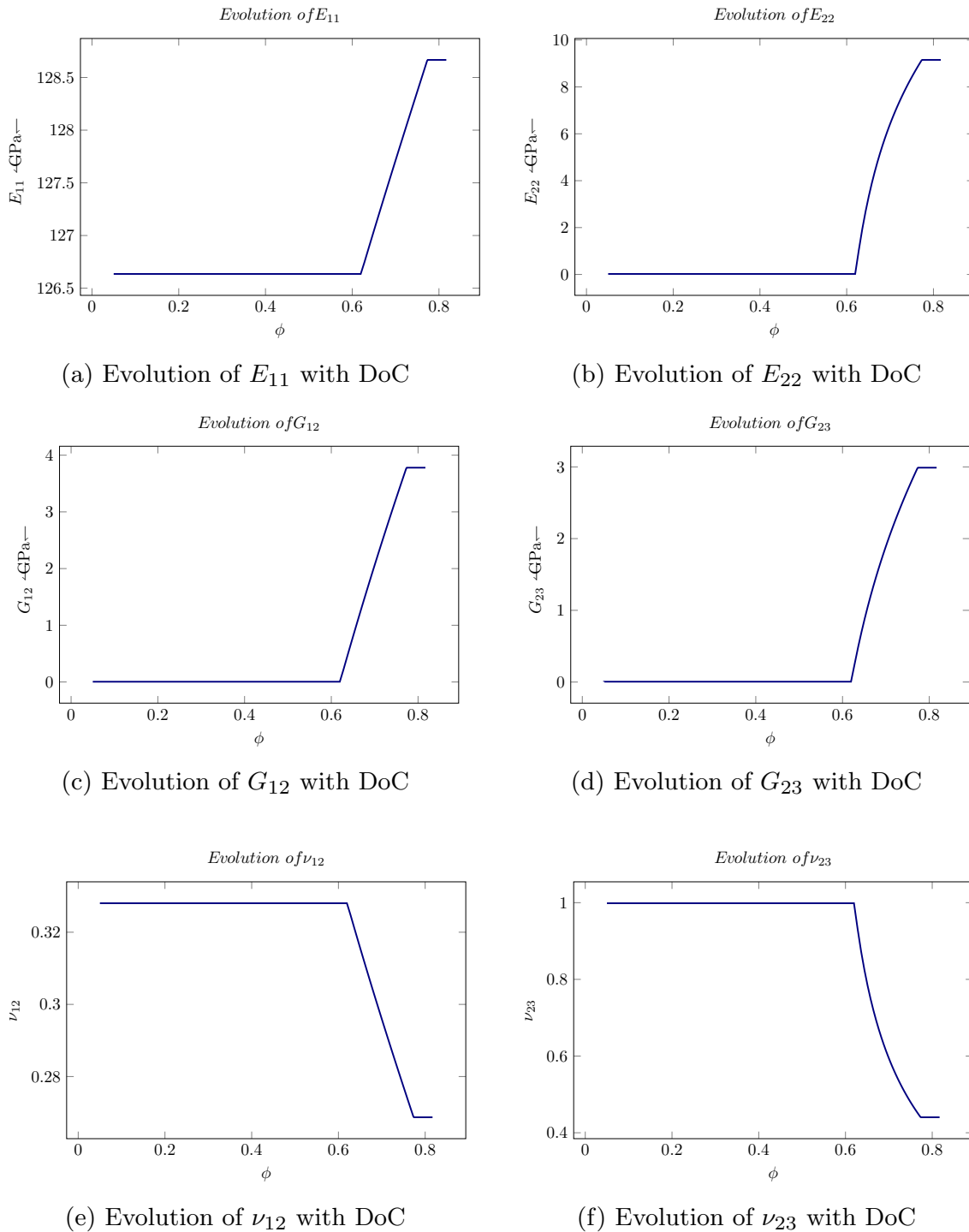


Fig. 13 Evolution of elastic constants with DoC for AS4/8552

material behavior assumption. The constructed surrogate models for σ_{11} and σ_{22} can be written explicitly as shown in Eq. (18) and Eq. (19), respectively. Here, both the equations are linear in temperature and quadratic in DoC.

$$\sigma_{11} = -24.71 - 0.41T + 727.96\phi + 0.03T\phi - 495.64\phi^2 \tag{18}$$

$$\sigma_{22} = -43.07 - 0.62T + 1215.53\phi + 0.11T\phi - 835.85\phi^2 \tag{19}$$

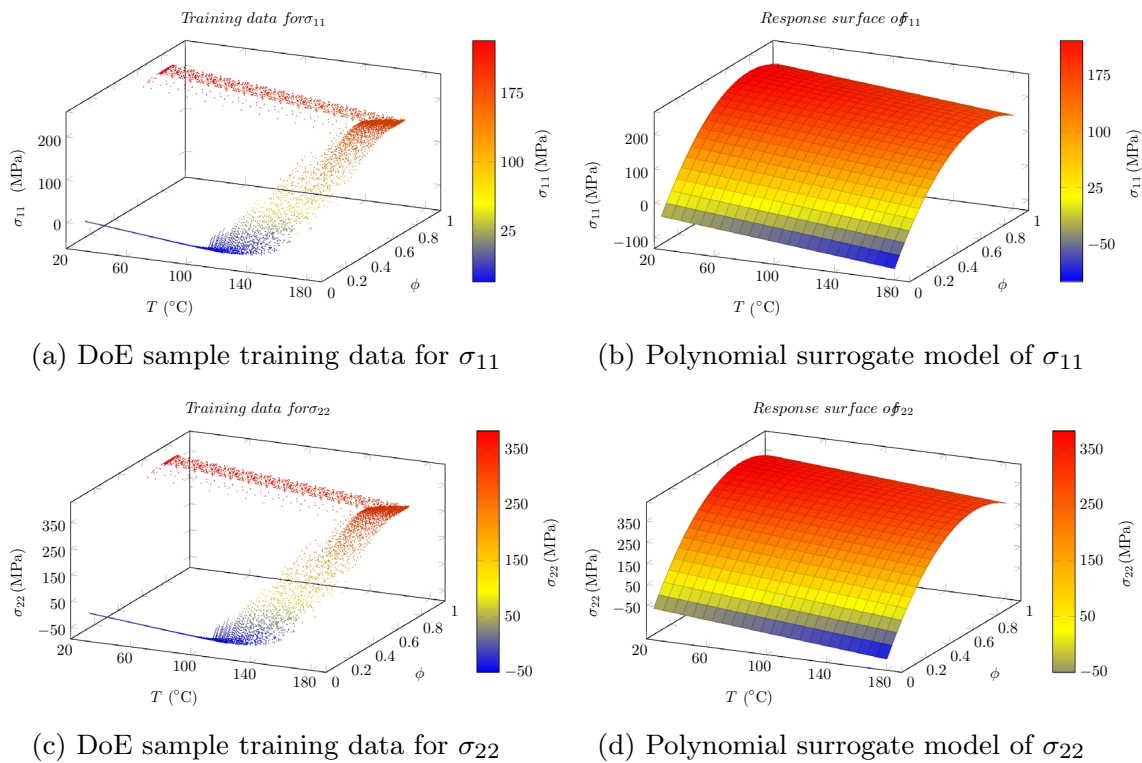


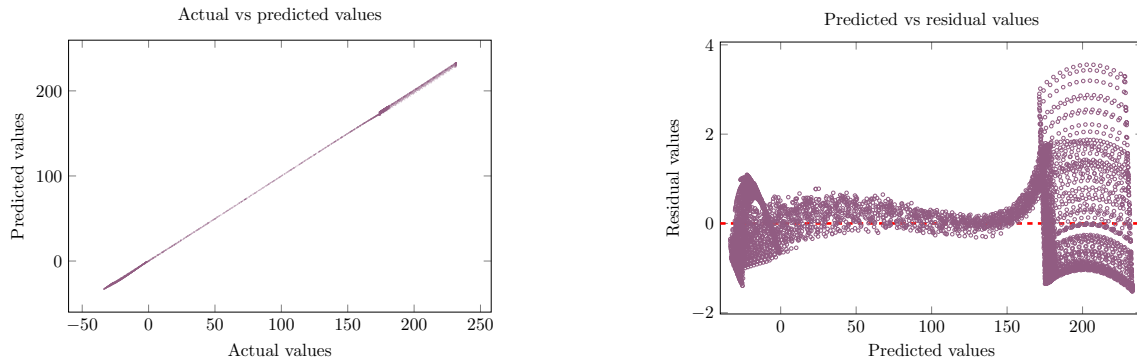
Fig. 14 Training data and surrogate model for micro-scale stresses

The constructed surrogate model needs to be validated with the training data to use them inside the USERMAT. Coefficient of determination or R^2 is commonly used in statistical community to validate the regression model. For both the σ_{11} and σ_{22} , R^2 value found to be 0.99 which is well beyond the accepted limit as surrogate model. Figure 15 shows the evaluation of surrogate model created for stress σ_{11} induced in AS4/8552 composite material. It is accurately able to predict the stress σ_{11} from the given temperature and degree of cure for any magnitude across the range as shown in Fig. 15b. The residual or error in surrogate model is negligible, and the frequency of high error is quite less as shown in Fig. 15c. The surrogate models of stress σ_{22} and σ_{33} are also able to predict with similar accuracy.

The manufacturer recommended cure cycle for given epoxy resin is a 2-step cycle as shown in Fig. 11. Where values of T_0 , T_1 , and T_2 are 25 °C, 107 °C, and 177 °C, respectively. Both heating rates are kept at 1 °C min⁻¹. Dwell times t_1 and t_2 have values of 1h and 2h. Figure 16 shows the DoC evaluation along with applied MRCC. Figure 17 shows the stress σ_{11} distribution near the corner in L-channel when MRCC is applied. The residual stress gets accumulated during the process due to cure shrinkage and thermal strains. The inner side of corner which is in contact with mold gets into tensile stress state while the outer side gets into compressive stress state. These stresses get

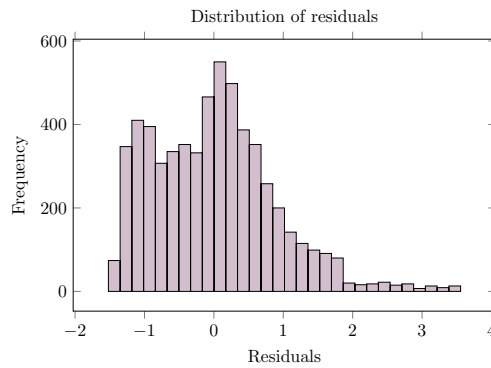
relieved after demolding and results into sping-in. This is undesirable and should be minimized along with process time.

The proposed multi-objective optimization algorithm, NSGA-II, is implemented in pymoo [44] which is based on Python programming language. The input bounds for the heat cycle are shown in Table 5. The NSGA-II algorithm's parameters used in the solution are shown in Table 6. This parameter combination requires a total of 360 FEA simulations. Each FEA requires about 10 min simulation time to simulate the outputs such as spring-in angle, process time, and DoC for the given temperature cycle. The entire FEA is carried out in on fifteen-core processor (2.8 GHz) Linux machine with 50 GB memory. The data points which encompass the objective function space with Pareto front are shown in Fig. 18; here, black marker represents the Pareto front (non-dominated solutions), and antique fuchsia marker shows the dominated feasible solutions. The objectives correspond to MRCC are also presented in Fig. 18. The points in the objective space are having the DoC of minimum and maximum value of 0.8 and 0.83, respectively. Two objectives studied here are conflicting in nature; increase in process time results in decrease in spring-in angle. In multi-objective optimization problem, there is no single unique best solution, but there is a set of Pareto-optimal solutions. Designer can select the any point on the Pareto front for the



(a) Actual vs predicted values

(b) Residual vs actual values



(c) Histogram of residual of surrogate model

Fig. 15 Evaluation of surrogate model for cure process induced stress σ_{11} for AS4/8552 composite material

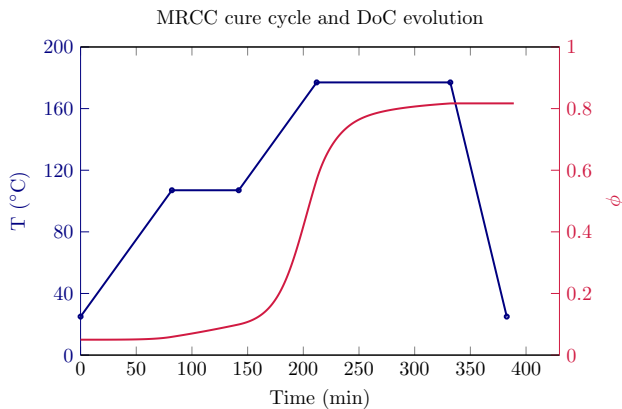


Fig. 16 MRCC cure cycle and corresponding DoC evolution

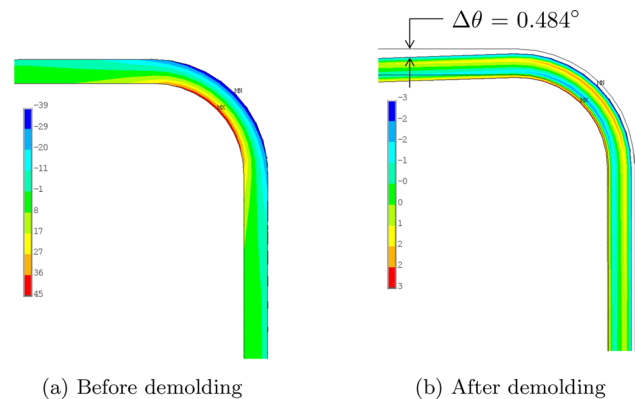


Fig. 17 Change in stress σ_{11} (MPa) for MRCC in composite L-channel

manufacturing of composite using, for example, weighted sum approach. Designer can provide the preference weight for each objective and select the points on the Pareto front. The process time for Pareto front is always lower than the MRCC results. The Pareto front and MRCC input and output values are reported in Table 7. Here, the table is ordered

Table 6 NSGA-II algorithm inputs

Parameter	Value
Population size	60
Number of offspring	10
Number of generation	31

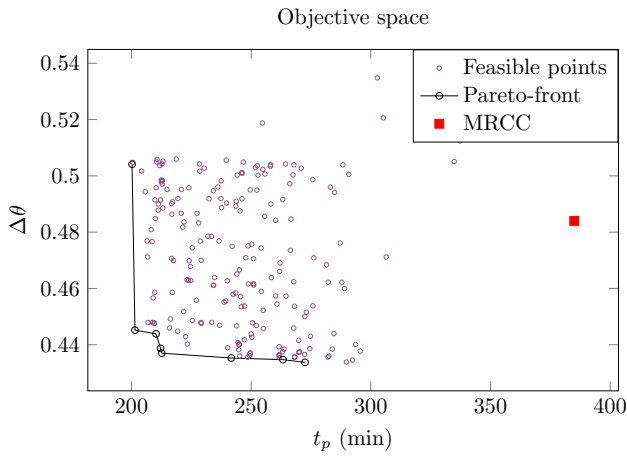


Fig. 18 Objective space with Pareto-front and MRCC

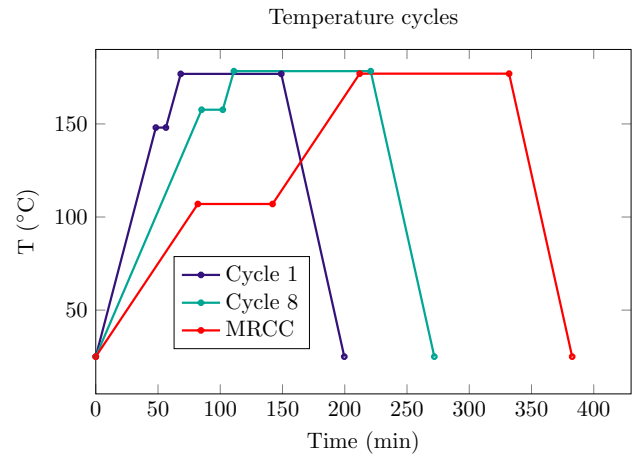


Fig. 19 Cure cycles for least process time, least spring-in angle, and MRCC

in increasing value of process time and enumerated from cycle 1 to cycle 8. If the manufacturer prefers least process time, cycle 1 can be selected, and if the manufacturer prefers least spring-in angle, cycle 8 can be selected. The cure cycle that corresponds to cycle 1, cycle 8, and MRCC are presented in Fig. 19. The corresponding DoC evolution for these cycles are shown in Fig. 20. Here, cycle 1 reaches saturation DoC early compared to cycle 8 and MRCC. It is observed that its first dwell period is smaller in general. The second dwell temperature for Pareto front is not changing significantly. The magnitude of improvement in spring-in angle over MRCC is smaller compared to process time. Pareto front gives the optimal solutions to select; however, the understanding relationship between inputs and outputs is necessary to understand the process effects. In these circumstances, parallel coordinates are useful. Figures 21 and 22 show the parallel coordinates to get lower process time and spring-in with DoC above 0.8, respectively. For both objectives, the first dwell period and second dwell temperature

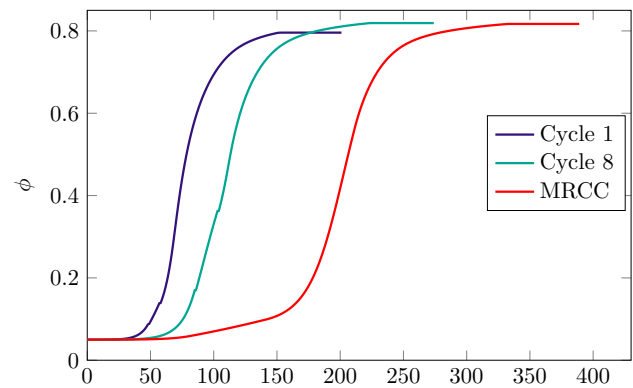


Fig. 20 Comparison of DoC evolution for three cycles: cycle 1, cycle 8, MRCC

are concentrated at lower and upper side of given range, respectively. The second dwell period for lower spring-in is observed to be higher.

Table 7 Inputs and output parameter of Pareto-front and MRCC

Cycle	t_1 (min)	t_2 (min)	T_1 (°C)	T_2 (°C)	q_1 (°Cmin ⁻¹)	q_2 (°Cmin ⁻¹)	t_p (min)	$\Delta\theta$ (°)	ϕ
1	8.09	80.75	148.94	176.87	2.55	2.42	200.21	0.504	0.801
2	7.90	82.26	158.36	177.37	2.80	1.56	201.44	0.445	0.806
3	12.54	80.81	147.54	177.34	2.24	2.78	210.25	0.444	0.804
4	18.55	82.26	158.36	177.42	2.80	1.56	212.13	0.439	0.809
5	18.55	81.85	158.36	178.37	2.80	1.56	212.65	0.437	0.813
6	40.30	80.81	153.50	178.77	2.24	2.24	241.64	0.435	0.816
7	23.32	117.46	139.36	178.57	2.15	2.25	263.28	0.435	0.824
8	17.01	109.87	157.63	178.35	1.56	2.32	272.49	0.434	0.822
MRCC	60	120	107	177	1	1	385	0.484	0.819

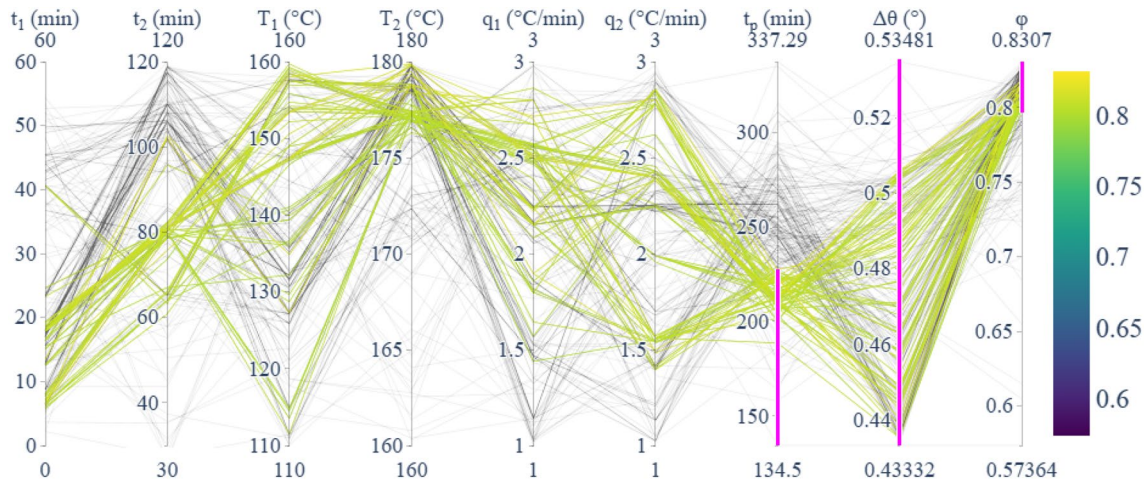


Fig. 21 Parallel coordinates for lower process time

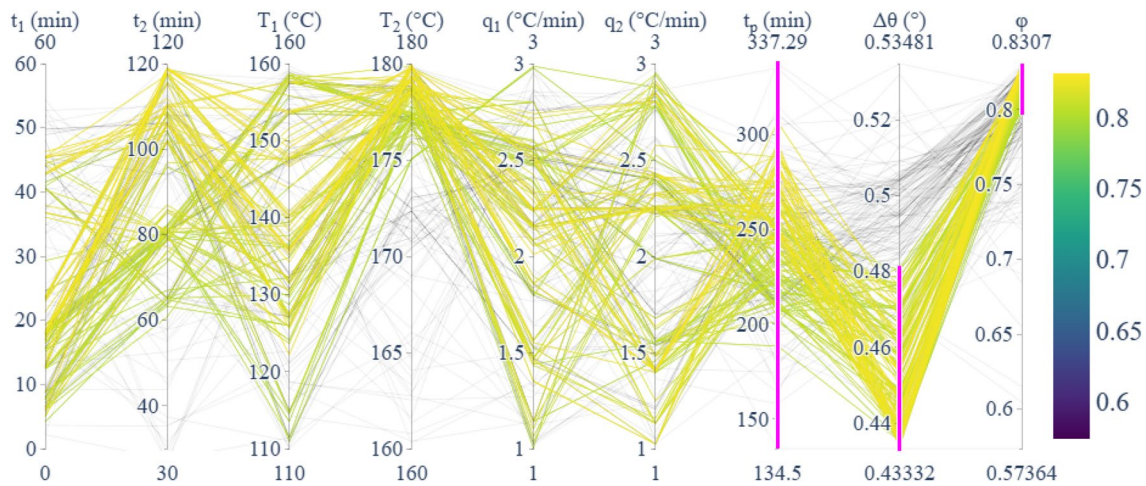


Fig. 22 Parallel coordinates for lower spring-in angle

Conclusions

In this study, the surrogate model based ICME approach is presented for the cure process analysis. Polynomial regression as surrogate model is used to predict the residual stresses due to cure shrinkage and thermal strains at micro-level. To generate the training data, Latin hypercube sampling is used to create multiple cure thermal cycles through parameterizing temperature cycle with six input variables. The corresponding cure cycles are applied to the micro-scale RVE model to extract the temperature, DoC, and residual stresses at specific intervals. The quadratic polynomial surrogate model is constructed for residual stresses as a function of temperature and DoC. The constructed quadratic polynomial surrogate model is able to predict the residual

stress accurately. Further, accuracy of the surrogate model is validated with the statistical R^2 metric. The proposed surrogate-assisted multi-scale methodology is implemented as a black-box simulation within NSGA-II for the optimization of the manufacturing process, with the primary objectives being the minimization of both the spring-in angle and the process time for composite L-channel part. The obtained results reveal significant improvements, with cycle 1 achieving a 48% reduction in process time. Furthermore, cycle 8 demonstrates notable advancements, achieving an 11% reduction in spring-in angle and a 29% reduction in process time. In addition, utilizing the data derived from the optimization process, parallel coordinates are generated to elucidate the connections between input variables and output responses. This approach facilitates comprehension of the

impacts of the process and contributes to informed decision-making. The advantages of the proposed surrogate assisted multi-scale approach are given as follows:

- The conventional approach is to homogenize cure shrinkage and thermal strain individually and to use them further to calculate stresses. The proposed approach of constructing surrogate model of stresses directly avoids the error propagation which may not be eliminated in aforementioned approach.
- The proposed approach does not need to summarize the constitutive laws similar to explicit multi-scale methods. Thus, it makes modeling cure process simulation through user subroutine simpler by including surrogate models of elastic constants and residual stresses.
- The approach is versatile similar to explicit multi-scale methods to include the other complex physics phenomena in model which might not be possible in general analytical methods.
- In addition, it is computationally efficient compared to explicit multi-scale method.

Nevertheless, it is important to acknowledge that, similar to any approach, the proposed methodology possesses certain limitations. While the surrogate-assisted multi-scale method proves to be computationally efficient for manufacturing process design, it necessitates that the input variable bounds used in surrogate model construction align with those utilized for process optimization. Deviations in these bounds may lead to inaccuracies in stress predictions by the surrogate models. Additionally, although NSGA-II is effective in identifying the Pareto front in process optimization, it demands a substantial number of function evaluations. Such an extensive computational burden becomes impractical when operating within constrained computational budgets. In forthcoming research endeavors, the objective is to present an integrated approach that combines optimization methods with high sample efficiency alongside surrogate-assisted multi-scale FEA. This unified approach holds the potential to substantially decrease the design cycle time throughout the initial stages of manufacturing process design.

Acknowledgements The authors express their sincere gratitude to Tata Consultancy Services for their generous support in conducting this research.

Declarations

Competing interests The authors declare that they have no known competing financial interests or personal relationships that could have appeared to influence the work reported in this paper.

References

1. Herakovich CT (1998) Mechanics of fibrous composites. Wiley, New York
2. Jones RM (2018) Mechanics of composite materials. CRC press
3. Tiwary A, Kumar R, Chohan JS (2022) A review on characteristics of composite and advanced materials used for aerospace applications. *Mater Today Proceed* 51:865–870
4. Sehgal AK, Juneja C, Singh J, Kalsi S (2022) Comparative analysis and review of materials properties used in aerospace industries: An overview. *Mater Today Proceed* 48:1609–1613
5. O'Brien DJ, Mather PT, White SR (2001) Viscoelastic properties of an epoxy resin during cure. *J Compos Mater* 35(10):883–904
6. Heinrich C, Aldridge M, Wineman AS, Kieffer J, Waas AM, Shahwan KW (2012) Generation of heat and stress during the cure of polymers used in fiber composites. *Int J Eng Sci* 53:85–111
7. Li X, Wang J, Li S, Ding A (2020) Cure-induced temperature gradient in laminated composite plate: numerical simulation and experimental measurement. *Compos Struct* 253:112822
8. White SR, Hahn H (1992) Process modeling of composite materials: residual stress development during cure. part ii. experimental validation. *J Compos Mater* 26(16):2423–2453
9. D'Mello RJ, Maiarù M, Waas AM (2015) Effect of the curing process on the transverse tensile strength of fiber-reinforced polymer matrix lamina using micromechanics computations. *Integrat Mater Manuf Innov* 4:119–136
10. Parthasarathy S, Mantell SC, Stelson KA (2004) Estimation, control and optimization of curing in thick-sectioned composite parts. *J Dyn Sys Meas Control* 126(4):824–833
11. Wang Q, Wang L, Zhu W, Xu Q, Ke Y (2020) Numerical investigation of the effect of thermal gradients on curing performance of autoclaved laminates. *J Compos Mater* 54(1):127–138
12. Kravchenko OG, Kravchenko SG, Pipes RB (2017) Cure history dependence of residual deformation in a thermosetting laminate. *Compos A Appl Sci Manuf* 99:186–197
13. Joosten MW, Agius S, Hilditch T, Wang C (2017) Effect of residual stress on the matrix fatigue cracking of rapidly cured epoxy/anhydride composites. *Compos A Appl Sci Manuf* 101:521–528
14. Albert C, Fernlund G (2002) Spring-in and warpage of angled composite laminates. *Compos Sci Technol* 62(14):1895–1912
15. He L, Zhao A, Li Y, Zhou B, Liang W (2021) Effect of processing method on the spring-in of aircraft ribs. *Compos Commun* 25:100688
16. Takagaki K, Minakuchi S, Takeda N (2017) Process-induced strain and distortion in curved composites. Part i: development of fiber-optic strain monitoring technique and analytical methods. *Compos Part A: Appl Sci Manuf* 103:236–251
17. Takagaki K, Minakuchi S, Takeda N (2017) Process-induced strain and distortion in curved composites. Part ii: parametric study and application. *Compos Part A: Appl Sci Manuf* 103:219–229
18. Kanouté P, Boso D, Chaboche J-L, Schrefler B (2009) Multiscale methods for composites: a review. *Archiv Comput Methods Eng* 16:31–75
19. Özdemir I, Brekelmans W, Geers M (2008) Fe² computational homogenization for the thermo-mechanical analysis of heterogeneous solids. *Comput Methods Appl Mech Eng* 198(3–4):602–613
20. Mahnken R, Dammann C (2016) A three-scale framework for fibre-reinforced-polymer curing part i: Microscopic modeling and mesoscopic effective properties. *Int J Solids Struct* 100:341–355
21. Chen W, Zhang D (2018) A micromechanics-based processing model for predicting residual stress in fiber-reinforced polymer matrix composites. *Compos Struct* 204:153–166

22. Zhi J, Yang B, Li Y, Tay T-E, Tan VBC (2023) Multiscale thermo-mechanical analysis of cure-induced deformation in composite laminates using direct Fe2. *Compos Part A: Appl Sci Manuf* 107704
23. Wang Q, Li T, Yang X, Huang Q, Wang B, Ren M (2020) Multiscale numerical and experimental investigation into the evolution of process-induced residual strain/stress in 3D woven composite. *Compos A Appl Sci Manuf* 135:105913
24. Yang Z (2001) Optimized curing of thick section composite laminates. *Mater Manuf Processes* 16(4):541–560
25. Carlone P, Palazzo GS (2011) A simulation based metaheuristic optimization of the thermal cure cycle of carbon-epoxy composite laminates. In: *AIP Conference proceedings*, vol. 1353, pp. 5–10. *Am Inst Phys*
26. Skordos AA, Partridge IK (2004) Inverse heat transfer for optimization and on-line thermal properties estimation in composites curing. *Inverse Problems Sci Eng* 12(2):157–172
27. Deb K, Pratap A, Agarwal S, Meyarivan T (2002) A fast and elitist multiobjective genetic algorithm: NSGA-II. *IEEE Trans Evol Comput* 6(2):182–197
28. Struzziero G, Skordos AA (2017) Multi-objective optimisation of the cure of thick components. *Compos A Appl Sci Manuf* 93:126–136
29. Dolkun D, Zhu W, Xu Q, Ke Y (2018) Optimization of cure profile for thick composite parts based on finite element analysis and genetic algorithm. *J Compos Mater* 52(28):3885–3894
30. Zhang W, Xu Y, Hui X, Zhang W (2021) A multi-dwell temperature profile design for the cure of thick cfrp composite laminates. *Int J Adv Manuf Technol* 117:1133–1146
31. Hui X, Xu Y, Zhang W, Zhang W (2022) Multiscale collaborative optimization for the thermochemical and thermomechanical cure process during composite manufacture. *Compos Sci Technol* 224:109455
32. Kamal MR (1974) Thermoset characterization for moldability analysis. *Polym Eng Sci* 14(3):231–239
33. Hubert P, Johnston A, Poursartip A, Nelson K (2001) Cure kinetics and viscosity models for hexcel 8552 epoxy resin. In: *International SAMPE symposium and exhibition*, pp. 2341–2354. *SAMPE*; 1999
34. Barbero Ever J (2013) finite element analysis of composite materials using ANSYS®. *CRC Press, Boca Raton*
35. Bogetti TA, Gillespie JW Jr (1992) Process-induced stress and deformation in thick-section thermoset composite laminates. *J Compos Mater* 26(5):626–660
36. Zobeiry N, Forghani A, Li C, Gordnian K, Thorpe R, Vaziri R, Fernlund G, Poursartip A (2016) Multiscale characterization and representation of composite materials during processing. *Philos Trans R Soc Mathe Phys Eng Sci* 374(2071):20150278
37. Johnston A, Vaziri R, Poursartip A (2001) A plane strain model for process-induced deformation of laminated composite structures. *J Compos Mater* 35(16):1435–1469
38. Fernlund G, Rahman N, Courdji R, Bresslauer M, Poursartip A, Willden K, Nelson K (2002) Experimental and numerical study of the effect of cure cycle, tool surface, geometry, and lay-up on the dimensional fidelity of autoclave-processed composite parts. *Compos A Appl Sci Manuf* 33(3):341–351
39. Kaszynski A pyansys: Python Interface to MAPDL and Associated Binary and ASCII Files. <https://doi.org/10.5281/zenodo.4009467>
40. Coello CAC, Lamont GB, Van Veldhuizen DA et al (2007) *Evolutionary algorithms for solving multi-objective problems*. Springer, Cham
41. Jain LK, Hou M, Ye L, Mai Y-W (1998) Spring-in study of the aileron rib manufactured from advanced thermoplastic composite. *Compos A Appl Sci Manuf* 29(8):973–979
42. McDowell DL, Panchal J, Choi H-J, Seepersad C, Allen J, Mistree F (2009) *Integrated design of multiscale, multifunctional materials and products*. Butterworth-Heinemann
43. Johnston AA (1997) *An integrated model of the development of process-induced deformation in autoclave processing of composite structures*. PhD thesis, University of British Columbia
44. Blank J, Deb K (2020) Pymoo: multi-objective optimization in python. *IEEE Access* 8:89497–89509

Springer Nature or its licensor (e.g. a society or other partner) holds exclusive rights to this article under a publishing agreement with the author(s) or other rightsholder(s); author self-archiving of the accepted manuscript version of this article is solely governed by the terms of such publishing agreement and applicable law.